

A Novel Multifocus Image Fusion Algorithm Based on Nonsubsampled Contourlet Transform

Cuiyin Liu^{1,2,3}, Peng Cheng^{1,2}, Shu-qing Chen¹, Cuiwei Wang⁴, Fenghong Xiang⁴

¹ College of Computer Science, Sichuan University Chengdu, Sichuan 610064 – China

[e-mail: liucuiyin@163.com, PeengCheng@163.com, talk2csq@hotmail.com]

² State Key Laboratory of Fundamental Science on Synthetic Vision Chengdu, Sichuan 610065 – China

[e-mail: liucuiyin@163.com, PeengCheng@163.com]

³ College of Computer Science, PanZhihua University PanZhihua, Sichuan 617000 – China

⁴ Computer Center, Kunming Univ. of Science and Tech.

[e-mail: 394116576@qq.com, xiangfh5447@sina.com]

*Corresponding author: Cuiyin Liu

Received June 5, 2012; revised December 26, 2012; accepted February 1, 2013; published March 29, 2013

Abstract

A novel multifocus image fusion algorithm based on NSCT is proposed in this paper. In order to not only attain the image focusing properties and more visual information in the fused image, but also sensitive to the human visual perception, a local multidirection variance (LEOV) fusion rule is proposed for lowpass subband coefficient. In order to introduce more visual saliency, a modified local contrast is defined. In addition, according to the feature of distribution of highpass subband coefficients, a direction vector is proposed to constrain the modified local contrast and construct the new fusion rule for highpass subband coefficients selection. The NSCT is a flexible multiscale, multidirection, and shift-invariant tool for image decomposition, which can be implemented via the à trous algorithm. The proposed fusion algorithm based on NSCT not only can prevent artifacts and erroneous from introducing into the fused image, but also can eliminate 'block effect' and 'frequency aliasing' phenomenon. Experimental results show that the proposed method achieved better fusion results than wavelet-based and CT-based fusion method in contrast and clarity.

Keywords: Image fusion; Multiresolution decomposition; multiscale; Nonsubsampled

1. Introduction

Due to the limited depth-of-focus of optical lenses in CCD devices, it is often not possible to get an image that contains all relevant objects within the depth of field. So, some objects are out of depth-of-focus and not clear. However, Some times people would like to acquire images that have large depth of field and accumulate more informative visual information for high layer of image processing, i.e., the images are in focus everywhere. One way to solve this problem is through image fusion, in which several images with different focus points are combined to form a clear image with all objects fully focused[1]. Image fusion can be defined as a process, in which a new image is produced by integrating complementary, multi-temporal or multi-view information from a set of source image without introduction of artifacts. In fusion process, all relevant and salient information of source image should be selected and transformed into the fused image[2]. However, in many situation, preprocess can not be perfectly satisfied. This unresolved problem leads to the various fusion algorithm to correct imperfection in fusion process. In recent years, image fusion has become an important research field in image analysis and computer vision.

The image fusion techniques can be divided into spatial-based domain and frequency-based domain two categories according to transform implemented on image or not[3]. Transform tool is used to realize the transformation from source image to frequency domain. In order to better present the visual information of image in frequency domain, various presentation measure of visual information for source image have been studied to get more effective fused result[4][5]. Excluding the presentation of the image, fusion rule is the another important technique for fusion quality, which is divided into pixel-level-based, feature-level-based, and decision-level-based. In fusion rule based feature-level, the coefficient selection of source image is combined with the feature of the image[6][7]. So we studied the better presentation of source image in transform domain, i.e.the multiscale decomposition tool, and selection rule of decomposed coefficients in this paper for improving fusion result.

2. Related Work

In spatial domain, a number of techniques for image fusion have been proposed with fusion operation directly on the source images, pixel-by-pixel. This method is simplest with average or maximum value fusion rule. However, this method would lead to many undesired effects, such as artifacts, blur edge and so on[8]. In order to meet the human visual system (HVS) and acquire more visual information in result, researchers have recognized that multiscale transform(MST) method are very useful for image fusion, and various mathematic MST-tools have been studied and used in image fusion[9][10][11][12]. The commonly used MST methods includes Laplacian pyramid(LP)[13], contrast pyramid [14], gradient pyramid, morphologic pyramid[15], and ration-of-low-pass pyramid[11]. The fusion algorithm on the transform domain is to perform a multi-scale transform on each source image firstly, and then employ fusion rule to select efficient feature to construct the composite image at this scale. The fused image is finally reconstructed by taking an inverse MST. The essence of the multiscale transform is to decompose the image into subband images at different resolution or scale. On the contrary, reconstruction is to combine these subband images to one composite image, which is the inverse of decomposition.

The better transform fully present the feature(i.e. salient features, edges,contourlet) of image, the less visual informaiton is lost in decomposition process. Recently, much research has been done. Many new multiscale transform tools, which can present source image in multiscale and multidirection, have been proposed and applied to the fusion algorithm, such as discrete wavelet transform(DWT)[16], contourlet transform(CT)[17]. These new methods can present source image in multi-direction and capture geometric structures of image.

However, DWT has serious limitations in image decomposition procedure, only three directions, which cannot preserve the salient features in source images very well and leads useful visual information of geometric to be lost. And then, DWT-based fusion scheme can not preserve the salient features in source images very well and will lead some 'block-effect' in the fused result. In the block of result image, geometrical inforamtion of image is lost, which leads zero gradient-value or no texture feature to be perceived by human eyes and low the image quality consequently.

With the further study of sparse representation, a theory for high dimensional signals called multiscale geometric analysis(MGA) has been developed. The contourlet transform is a multidirectional and multiscale transform which is constructed by combining Laplcian pyramd(LP) with driectional filter bank proposed in [19]. Furhermore, the number of directions can be defined by i -th power of 2, where i is an arbitrary natural number in theory selected by need. In the contourlet transform, the LP is employed to capture the point discontinuities, and then followed by direction filter banks(DFB) to link discontinuities into linear structure [25]. Compared with the DWT, the CT can capture 2-D geometrical structures much more effectively than traditional multiresolution analysis methods.

Due to downsamplers and upsamplers present in decomposition, the contourlet transform is not shift-invaraint, which is desirable in many image applications such as image enhancement, image denoising and image fusion. An example that illustrate the importance of shift-invaraince is image denoising by threshold, where the lack of shift-invariance causes pseudo-Gibbs phenomean around singularities[20]. So, shift-invariance, it has been considered to be an effective representation to account for the geometrical structure pervasive in natural scenes. In 2006, Cunha,et al. proposed the nonsubsamped contourlet transform(NSCT) based on contourlet transform[18]. The NSCT is a fully shift-invariant, multi-scale and multi-direction expression and has a fast implementation. After decomposition, subband image has the same size as source image, which is easy for the coefficients selection operation.

In this paper, a novel image fusion algorithm based on the NSCT is proposed. Especially, according to the imaging principle of the defocused optical system, the feature of the human vision system and feature of coefficients decomposed by NSCT, the selection principles of the lowpass subband coefficients and the bandpass directional subband coefficients are discussed in detail, several group of experimental results are employed to demonstrate the great validity and feasibility of the proposed algorithm. The rest of the paper is organized as follows: Section 3 reviews the theory of the NSCT in brief. Section 4 describes the novel fusion algorithm using the NSCT. Experimental results and analysis are given in Section 5. The concluding remarks are presented in Section 6.

3. Nonsampled Contourlet Transform

The nonsampled DFB is a shift-invariant version of the sampled DFB in the contourlet transform. In order to get rid of the frequency aliasing of the contourlet transform (CT), the nonsampled contourlet transform (NSCT) based on nonsampled pyramid filter and nonsampled directional filter banks provide a shift-invariant multi-direction and multi-resolution presentation of image was proposed by Arthur L. da Cunha et.al.[20]. In this section, we briefly introduce the new multi-scale decomposition tool and analyze the feature of the image coefficient decomposed by NSCT. The structure of nonsampled contourlet transform is shown in Fig. 1 (a), and frequency partitioning result is shown in Fig. 1(b).

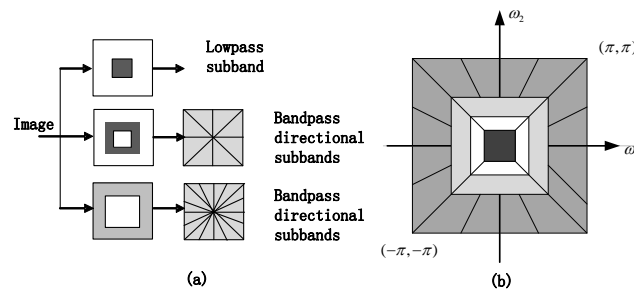


Fig. 1. Nonsampled contourlet transform: (a)NSFB structure that implements the NSCT and; (b)idealized frequency partitioning obtained with the proposed structure

3.1 Nonsampled Pyramid(NSP)

Laplacian pyramid(LP) is used for attaining multiscale decomposition in contourlet transform(CT). While in NSCT, the modified Laplacian pyramid is employed for multiscale decomposition, which is composed of two-channel nonsampled 2-D filter bank. In decomposition process, upsampling filter bank is used to ensure the shift-invariance. Accordingly, downsampling filter bank is used in reconstruction process. The filtering with the upsampled filter $H(z^M)$ is computed with the ‘àtrous’ algorithm [22]. The equivalent filters of a 3-th level cascading nonsampled pyramid decomposition is given by Fig.2.

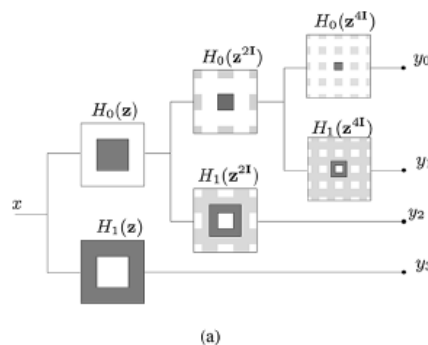


Fig. 2. Three-stage pyramid decomposition.

3.2 Nonsampled Directional Filter Bank(NSDFB)

The DFB is composed of combining critically sampled two-channel fan filter banks and resampling operations, which results in a tree-structured filter bank that splits the 2-D frequency plane into directional wedges[23]. In NSCT, a shift-invariant directional expansion is obtained with a nonsampled DFB(NSDFB), which is constructed by

eliminating the downsamplers and upsamplers in the DFB. To obtain finer directional decomposition, we iterate nonsubsampled DFB's. Fig. 3 illustrates a decomposition process with four channels. All filter banks in the nonsubsampled directional filter bank tree structure are obtained from a single NSF with fan filter. Moreover, each filter bank in the NSDFB tree has the same computational complexity as that of the building-block NSF.

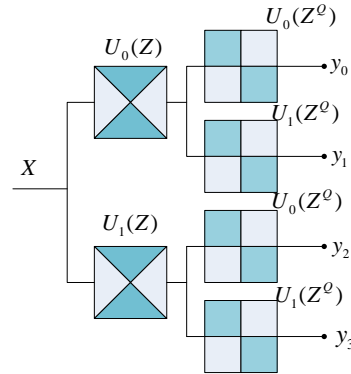


Fig. 3. Four-channel NSDFB constructed with two-channel fan filter bank:(a) iterated nonsubsampled directional filter bank structure (b)corresponding frequency partitioning.

The NSCT not only present source image in multiscale and multidirection, but also eliminate the aliasing by using NSP and NSDFB, which can capture the geometric features such as edges, lines, region boundaries, and so on. In image fusion research, the multi resolution decomposition is a key component for improving the fusion quality.

4. The proposed Fusion Algorithm

4.1 The proposed Fusion Algorithm

A good image fusion algorithm can preserve all salient features in source images and introduce as less artifacts or inconsistency as possible [24]. In the following work, it has been assumed that the images studied has been appropriately preregistered, so that corresponding pixel position roughly consistency and help to the coefficients selection in fusion process. I^A and I^B denotes the source image. The fusion result is a composite image I^F from I^A and I^B by using fusion rule. The frame of fusion algorithm is described as the follows steps:

Firstly, the source images I^A and I^B are decomposed by the NSCT to an approximation lowpass subband coefficient and a number of directional subband coefficients respectively.

$$I^A \rightarrow C_0^A, C_{1,1}^A, C_{1,2}^A, \dots, C_{l,d}^A$$

$$I^B \rightarrow C_0^B, C_{1,1}^B, C_{1,2}^B, \dots, C_{l,d}^B$$

Where C_0^A, C_0^B denotes the lowpass subband coefficient at the coarsest scale. $C_{l,d}^A(m, n)$ denotes the directional subband coefficients at the l -th scale, d -th direction.

Secondly, the low subband coefficient is selected from the lowpass coefficient of C_0^A and C_0^B according to lowpass fusion rule. Similarly, the highpass subband coefficients are selected from the directional coefficients of $C_{l,d}^A(m, n)$ and $C_{l,d}^B(m, n)$ according to highpass fusion rule.

Finally, the fused image I^F is obtained by reconstructing the selected coefficients inversely.

In fusion algorithm, apart from using the proper multiscale decomposition tool, the fusion rule is another key component for improving fusion quality. In order to achieve better visual results, a novel fusion rule is proposed in this section. The design of fusion rule for lowpass subband and highpass subbands is considered in next context, respectively.

4.2 The Fusion Rule of Lowpass Subband Coefficient

Lowpass subband coefficient is approximate representation of the image, including major energy and contours of the image. A simple lowpass subband coefficient fusion method is to take the average of two source coefficient. However, when the method is applied, contrast of features is reduced. In order to solve this problem, several measures and features selection rule have been studied and used in the previous studies[26]. such as spatial frequency(SF), energy of image gradients(EOG), which were introduced by Eskicioglu and Fishier as clarity measure of image. SF is defined as

$$SF = \sqrt{(RF)^2 + (CF)^2} \quad (4)$$

Where RF is the row frequency,

$$RF = \sqrt{\frac{1}{M \times N} \sum_{i=1}^M \sum_{j=2}^N [I(i, j) - I(i+1, j)]^2} \quad (5)$$

CF is column frequency.

$$CF = \sqrt{\frac{1}{M \times N} \sum_{j=1}^M \sum_{i=2}^N [I(i, j) - I(i, j+1)]^2} \quad (6)$$

Energy of image gradient (EOG) is computed as

$$EOG = (I_x)^2 + (I_y)^2 \quad (7)$$

Where

$$I_y = I(i+1, j) - I(i, j), I_x = I(i, j+1) - I(i, j) \quad (8)$$

The energy of gradient represents the clarity and sharpness of an image. Feature of image presented by adjacent region of current pixel is more fit for human visual system. So the local energy of gradient (LEOG) is adopted, which is defined as follows:

$$LEOG(i, j) = \sum_{p=-(w-1)/2}^{(w-1)/2} \sum_{q=-(w-1)/2}^{(w-1)/2} (I_x(i+p, j+q))^2 + (I_y(i+p, j+q))^2 \quad (9)$$

Where, w is the size of local window, which can be $3 \times 3, 5 \times 5, 7 \times 7$.

SF and EOG measure is actual filtered result in horizontal and vertical directions. Considering the limited direction, we use the energy of multidirection variance of image(EOV) as the measure of image clarity enlightened by the idea of energy of Laplacian (EOL)[1]. Similarly, we use the local EOV(LEOV) to represent the feature of image. The energy of image local multi-direction variance of image (LEOV) is defined as Eq.(10),which can represent more edges information than the energy measure.

$$LEOV(i, j) = \sum_{p=-(w-1)/2}^{(w-1)/2} \sum_{q=-(w-1)/2}^{(w-1)/2} I_x^2(i+p, j+q) + I_y^2(i+p, j+q) + I_d^2(i+p, j+q) \quad (10)$$

where, w is the size of local region. I_x, I_y and I_d is attained by convolving the image I with operators h_x, h_y, h_d respectively.

$$I_x = I * h_1, h_1 = [-1, -1, -1; 2, 2, 2; -1, -1, -1]$$

$$I_y = I * h_2, h_2 = [-1, 2, -1; -1, 2, -1; -1, 2, -1]$$

$$I_d = I * h_d, h_d = [-1, 0, -1; 0, 4, 0; -1, 0, -1]$$

Let $LEOV^A(i, j)$ and $LEOV^B(i, j)$ denote feature of the lowpass subband coefficient of image I^A and I^B . the selection principle for the lowpass subband coefficients is finally defined as

$$I^F(x, y) = \begin{cases} I^A(x, y) & \text{if } LEOV^A(i, j) \geq LEOV^B(i, j) \\ I^B(x, y) & \text{if } LEOV^A(i, j) < LEOV^B(i, j) \end{cases} \quad (11)$$

The selection rule is to select the coefficient with maximum LEOV as fusion coefficients, which means more direction energy and more visual information are introduced into the fusion image.

4.3 Selection of Bandpass Directional Subband Coefficients

The directional subband coefficients directionally represent the details of source image, such as the edges, contours, and object boundaries. In order to keep the salient feature in the fusion image, the multiresolution coefficients with larger absolute values generally be considered correspond to pixels with sharper brightness in the image, which will be selected into the fusion result. Other similar coefficient selection measure represented for the salient feature of image is used to improve the fusion quality, in which including energy of image, gradient energy of image, Laplacian energy of image. At the same time, research has been done in [27] shown that human visual system is highly sensitive to the local image contrast. The pixel with high contrast value is more liable to attract human attention. So, local contrast is used in fusion rule to select pixel with maximum local contrast as result.

Based on the analysis from above contents, we propose a novel fusion rule for highpass subband. Firstly, not only in order to preserve the saliency but also be sensitive to human visual system, a modified local contrast is defined for accomplishing it. Secondly, based on analyzing feature of coefficient decomposed by NSCT, a direction vector is proposed and combined with the modified local contrast to construct the finally selection principle for highpass subband coefficients.

According to the HVS, the contrast was proposed by Toet and Ruyven in [24]. It defined as

$$R = \frac{L - L_B}{L_B} = \frac{\Delta L}{L_B} \quad (12)$$

where L denotes the local gray level, L_B is the local brightness of the background and corresponds to the low frequency component. Generally, ΔL corresponds to local high frequency component. In NSCT domain, ΔL is the directional subband coefficient. So the direction contrast is defined as follows.

$$Con_{l,d}(i, j) = \begin{cases} \frac{|C_{l,d}(i, j)|}{I_l(i, j)}, & I_l(i, j) \neq 0 \\ |C_{l,d}(i, j)|, & I_l(i, j) = 0 \end{cases} \quad (13)$$

Among, $C_{l,d}(i, j)$ is the coefficient in l -th layer and d -th direction. $I_l(i, j)$ is often replaced by the corresponding lowpass coefficient C_0^A , C_0^B . In order to introduce the saliency into the local contrast, we modified the $C_{l,d}(i, j)$ according to the idea mentioned in [24] and construct the new direction contrast, which is calculated as Eq.(14).

$$Con_{l,d}(i, j) = \begin{cases} \frac{|MSLC_{l,d}(i, j)|}{I_l(i, j)}, & I_l(i, j) \neq 0 \\ |MSLC_{l,d}(i, j)|, & I_l(i, j) = 0 \end{cases} \quad (14)$$

Where,

$$MSLC_{l,d}(i, j) = |8I^{l,d}(i, j) - 4I^{l,d}(i-1, j) - 4I^{l,d}(i+1, j)| + |8I^{l,d}(i, j) - 4I^{l,d}(i, j-1) - 4I^{l,d}(i, j+1)| \\ + 2I^{l,d}(i, j) - I^{l,d}(i-1, j+1) - I^{l,d}(i+1, j-1)| + |2I^{l,d}(i, j) - I^{l,d}(i-1, j-1) - I^{l,d}(i+1, j+1)|$$

Human visual system sensitive to salient features, but insensitive to the feature of single pixel. So, a pure use the contrast of single pixel is not effective idea. It will be more reasonable to replace the contrast of single pixel with the local contrast. Local direction contrast is defined as follows.

$$LCon_{l,d} = \sum_{p=-(w-1)/2}^{(w-1)/2} \sum_{q=-(w-1)/2}^{(w-1)/2} Con_{l,d}(i+p, j+q) \quad (15)$$

Where w is the size of local region

The local direction contrast represents the salient features of image more accurately and to select coefficients from the clear parts successfully. At the same time, the noise is introduced into the fused coefficient. In NSCT domain, the decomposed coefficients is different from another multiresolution decomposed coefficients. The noise and the useful information of source image decomposed by NSCT have the different distribution in directional coefficients.

The nonsubsampling contourlet transform not only provides multiresolution analysis, but also geometric and directional representation [28][29]. An important result is that the highpass subband coefficients were divided into three classes: strong edges, weak edge, and noises. The strong edges corresponds to those pixels with big-value coefficients in all subbands. The weak edges corresponds to those pixels with big-value coefficients in some directional subbands but small-value coefficients in other directional subbands within the same scale. The noise corresponds to those pixels with small-value in all directional subbands. From these analysis, coefficients can be classified three categories by analyzing the distribution of themselves in different directional subbands. The classified way is defined as follow.

$$\begin{cases} \text{strong edge} & \text{if } mean \geq c\sigma \\ \text{weak edge} & \text{if } mean < c\sigma, \max \geq c\sigma \\ \text{noise} & \text{if } mean < c\sigma, \max < c\sigma \end{cases} \quad (16)$$

Where c is a parameter ranging from 1 to 5, and σ is noise standard deviation of the subbands at a specific level. The noise can be distinguished by the directional coefficients. So we can use this merits in fusion procedure to eliminate the noise. A vector directional $v_l(i, j)$ at l -th scale and location (i, j) is defined as equation 17.

$$v_l(i, j) = (C_{l,1}(i, j), C_{l,2}(i, j), \dots, C_{l,d}(i, j))^T, l \geq 0 \quad (17)$$

Where $C_{l,d}(m, n)$ is the directional subband coefficient at the l -th scale and d -th direction, d is the number of decomposed direction at this scale. The absolute sum of directional vector is defined as

$$s_l = \sum_{d=1}^d |C_{l,d}(m, n)| \quad (18)$$

From the above analysis, The proposed fusion rule constrained by directional vector and local contrast(VLCON) is finally defined as follows:

$$F_{ld}^F(i, j) = \begin{cases} C_{ld}^A(i, j) & s_l^A \cdot LCon_{l,d}^A(i, j) \geq s_l^B \cdot LCon_{l,d}^B(i, j) \\ C_{ld}^B(i, j) & s_l^A \cdot LCon_{l,d}^A(i, j) < s_l^B \cdot LCon_{l,d}^B(i, j) \end{cases} \quad (19)$$

The $MSCL$ used in Local contrast is the sum of modified Laplacian, which is used to analyze high frequencies associated with image edges. In application, the larger value of $MSCL$, the more edges information. We adopt $MSCL$ as feature of highpass subbands to replace the single pixel value in the contrast measure for fusing more edges information to the result. At the same time, the sum of direction vector s_l is used together with $LCON$ to construct highpass fusion measure. The larger value s_l of the pixel, the smaller possibility value of noise. The pixel with higher s_l and $LCon_{l,d}$ values is more likely to correspond to important visual information. The proposed fusion rule for highpass subbands cannot only extract more useful visual detailed information from source images and inject them into the fused image,

but also sensitive to the human visual system. Furthermore, the absolute sum of direction vector is used in selection scheme to prevent the noise being transferred into the fused image.

5. Experimental Classification Results and Analysis

In order to show the advantages of the new fusion method, Four sets of experiments were carried out for multifocus image fusion to demonstrate the advantages of the proposed algorithm.

Firstly, in order to compare performance of the various lowpass subband fusion rule with other conventional fusion rule[3][4][5], a variety of lowpass subband fusion rule is experimented. In these experiments, the highpass subband coefficients are simply merged by the ‘local energy maximum’ choosing scheme.

Secondly, in order to demonstrate the effectiveness of highpass subband coefficients fusion rule proposed in this paper, experiments for comparing it with other conventional fusion rule [3][4][5] are carried. In all of which the lowpass subband coefficients are simply merged by the ‘average scheme’.

Finally, in order to demonstrate the proposed fusion algorithm outperform other fusion algorithm, the proposed fusion algorithm is compared with other typical fusion algorithms including DWT-based algorithm[5], CT-based algorithm[21],NSCT-based algorithm[4].

5.1 Comparisons of fusion rule in Lowpass Subband

The fusion experiments are performed using fusion rule in lowpass subband for coefficient selection, including ‘average scheme’, ‘directional vector maximum choosing scheme’, ‘local gradient energy maximum choosing scheme’, ‘and local multi-direction variance (LEOV) maximum scheme’. At the same time the highpass subband coefficient is selected by ‘abs-max’ scheme in the above experiments.

In **Fig. 4** The experiments are performed on the multifocus ‘bookshelf’ images which shown in **Fig. 4 (a)** and **(b)**. The pseudo-edge is exist near the white book in **Fig. 4 (c)-(d)** and not in **Fig. 4 (e)-(f)**. In order to observer the local fusion details of the fusion image, we take part image of the book from the **Fig. 4 (c)-(f)** and enlarge the part in Fig.5 for observation. The blur edges and information lost is existed in **Fig. 5 (a)-(b)**. Pseudo-edge and the shadow are present near the book contour. Especially in **Fig. 5 (c)**, information lost is so serious that writing and edges of the book can’t be identified. Better visual quality with clear details and close to the real natural images is obtained in **Fig. 5 (c)-(d)**. **Fig. 5 (c)** is fused by NSCT and with average-value method in lowpass image and maximum-value method in highpass image. **Fig. 5(d)** is the fused result by proposed fusion rule. Because the energy of local multi-direction variance can transform more edges information to fused result, The shift-invariance of NSCT eliminate the ‘pseudo-edge’ effectively, So, **Fig. 5 (d)** is more clear than **Fig. 5 (c)**, and the edges are more natural than that of **Fig. 5 (c)**.



Fig. 4. The fusion results of different lowpass coefficient fusion algorithms: (a) Focus on the right; (b) focus on the left; and (c)–(f) fused images using the average scheme, directional vector maximum choosing scheme, local gradient energy maximum choosing scheme, and the proposed lowpass subband fusion rule.

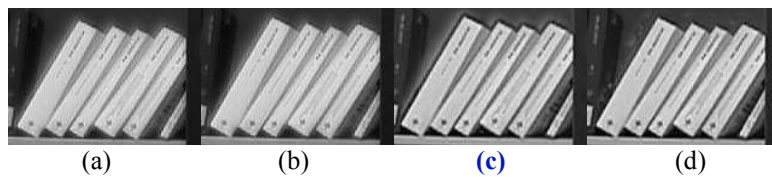


Fig. 5. Parts of the fusion images: Fig.6:(a)–(e) taken from Fig.5(c)–(f), respectively.

For further comparison, besides visual observation, mutual information (MI)[29]. The information preservation value for edges denoted by $Q^{AB/F}$ [30] metric and spatial frequency metric are used to evaluate the fusion performance quantitatively. The mutual information metric denotes how much information from source images was introduced to the fused image. The mutual information[31] M_F^{AB} between the source image A, B and the fused image F is defined as the sum of I_{AF} and I_{BF} , i.e. $M_F^{AB} = I_{AF} + I_{BF}$. where I_{AF} and I_{BF} indicates the mutual information between fused image and the source image A and B respectively. I_{AF} is

defined as

$$I_{AF} = \sum p_{AF} \log \frac{p_{AF}}{p_A p_F} \quad (20)$$

Where p_A and p_F is the normalized histogram of A and F, respectively. p_{AF} is the normalized joint histogram of image A and F, and I_{BF} is defined similarly.

The $Q^{AB/F}$ metric denotes how much edges information is transferred from input images to the fused image. This method uses a Sobel edge detector to calculate the strength and orientation information at each pixel in both source and fused image. For two input images A and B, $Q^{AB/F}$ is defined as

$$Q_p^{AB/F} = \frac{\sum_{n=1}^N \sum_{m=1}^M Q^{AF}(n,m)w^A(n,m) + Q^{BF}(n,m)w^B(n,m)}{\sum_{i=1}^N \sum_{j=1}^M (w^A(i,j) + w^B(i,j))} \quad (21)$$

$Q^{AF}(n,m)$, $Q^{BF}(n,m)$ is the value of edges information preservation, which is defined as: $Q^{AF}(n,m) = Q_g^{AF}(n,m)Q_\alpha^{AF}(n,m)$, where $Q_g^{AF}(n,m)$ is edge strength, $Q_\alpha^{AF}(n,m)$ is orientation preservation value.

$$Q_g^{AF}(n,m) = \frac{\Gamma_g}{1 + e^{k_g(G^{AF}(n,m) - \sigma_g)}} \quad (22)$$

$$Q_\alpha^{AF}(n,m) = \frac{\Gamma_\alpha}{1 + e^{k_\alpha(G^{AF}(n,m) - \sigma_\alpha)}}$$

The relative strength and orientation values of $G^{AF}(m,n)$ and $A^{AF}(n,m)$ of input image A with respect to F are formed as

$$G^{AF}(n,m) = \begin{cases} \frac{g_F(n,m)}{g_A(n,m)}, & \text{if } g_A(n,m) > g_F(n,m) \\ \frac{g_F(n,m)}{g_A(n,m)}, & \text{otherwise} \end{cases} \quad (23)$$

$$A^{AF}(n,m) = \frac{|\alpha_A(n,m) - \alpha_F(n,m)| - \pi/2}{\pi/2}$$

Where,

$$g_A(n,m) = \sqrt{s_A^x(n,m)^2 + s_A^y(n,m)^2}$$

$$\alpha_A(n,m) = \tan^{-1}\left(\frac{s_A^y(n,m)}{s_A^x(n,m)}\right)$$

Where, $g_A(n,m)$ is edge strength, $\alpha_A(n,m)$ is orientation information. all of them are generated by the sobel edge operator for each pixel $p(n,m)$ $1 \leq m \leq M$ and $1 \leq n \leq N$.

Table 1. Performance of the different lowpass subband fusion rule on processing Fig.4.

Fusion rule	Mutual information	Q^{AF}	Q^{BF}	$Q^{AB/F}$	SF
Average	5.906	11.463	11.463	0.5615	5.027
Directional vector	5.906	11.463	11.463	0.5615	5.017
LEOG	7.031	11.442	11.442	0.7127	6.001
LEOV	7.454	11.378	11.378	0.7164	5.938

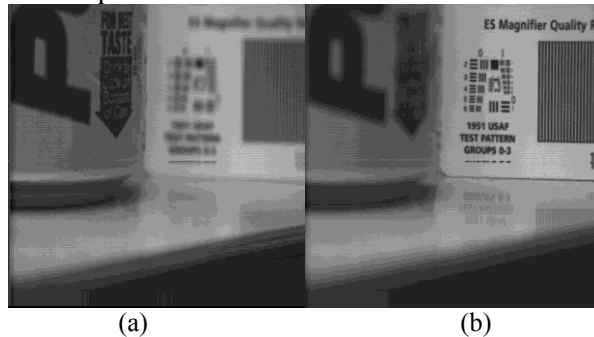
Furthermore, objective criteria on mutual information (MI) and $Q^{AB/F}$ in **Table 1** indicate that our proposed fusion rules of the low frequency subband are very useful for fusion of multifocus clean images.

5.2 Comparisons of Highpass Subband Fusion Rule

The second experiment is performed on ‘pepsi’ images registered beforehand. The focus in **Fig. 6(a)** is on the Pepsican, while the focus in **Fig. 6 (b)** is on the card. Fusion results of different kinds highpass fusion rules are shown in **Fig. 6 (c)-(d)**. The ‘local contrast maximum scheme’, ‘local energy maximum scheme’, ‘the local variance maximum scheme’ and the proposed fusion rule are implemented for highpass subband coefficients selection, respectively. Amongst these lowpass subband fusion process, ‘average scheme’ is used for all. The results of fusion experiments are shown in **Fig. 6 (c)-Fig.6(f)**.

For a clearer comparison and better illustrate effectiveness of the proposed fused method, the difference between the fused image and the source image focus on right (in **Fig. 6 (b)**) are shown in **Fig. 6 (g)-(h)**, respectively. **Fig. 6 (b)** is focus on right, which means the right part is clear. The ideal difference of this part between the fused image and the **Fig. 6 (b)** should be zero. The smaller the difference, the better the fusion algorithm. From the **Fig. 6 (g)** to **Fig. 6 (j)**, one can obviously find that the fused image obtained by the proposed method is clearer than the other fusion methods for the difference value of this part is smallest. It is proven that the proposed fusion rule of the highpass subband coefficient is reasonable and can extract more useful information from source images.

Quantitative comparison of their performance are given in **Table 2**, which indicate that our proposed fusion rules of highpass subbands are very useful. Obviously, the maximum values of MI, and $Q^{AB/F}$ and SF demonstrate that the proposed method transfer more edge information to the fused images. So we can conclude that the proposed highpass subband fusion rule provides the best performance than conventional others.



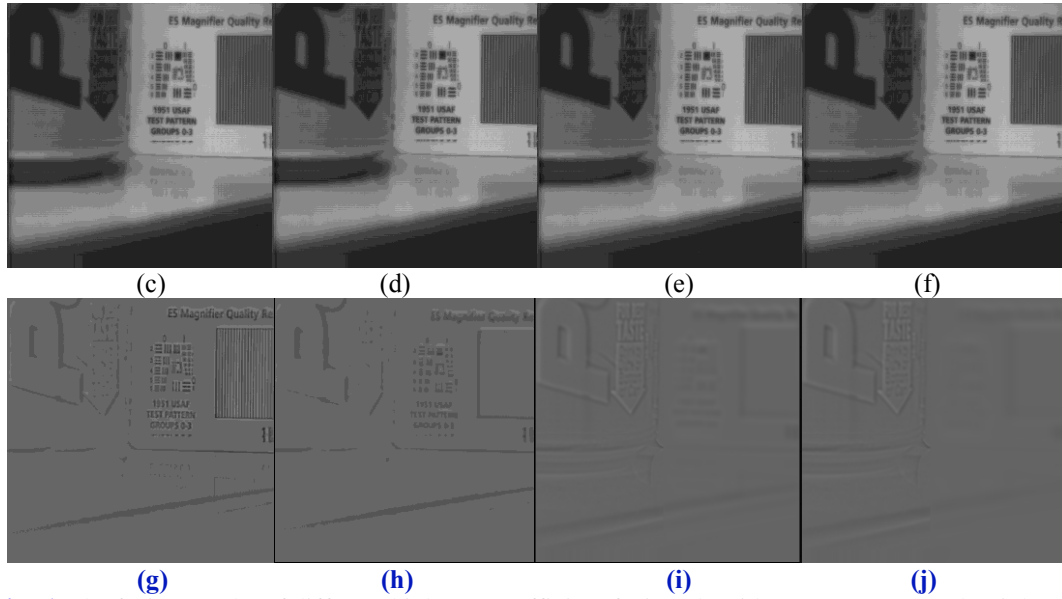


Fig. 6. The fusion results of different highpass coefficient fusion algorithms: (a) Focus on the right; (b) focus on the left; and (d)–(f) fused images using ‘local contrast maximum scheme’, ‘local energy maximum scheme’, ‘the local variance maximum scheme’ and the proposed fusion rule. (g)–(j) Difference images between Fig.6(c)–(f) and Fig.6(b), respectively.

Table 2. Performance of the different highpass subband fusion rule on processing Fig.6.

Fusion rule	Mutual information	Q^{AF}	Q^{BF}	$Q^{AB/F}$	SF
Local contrast	6.701	10.847	10.847	0.660	4.742
Local energy	6.700	10.852	10.852	0.660	4.745
Local variance	6.700	10.852	10.853	0.660	4.742
Proposed	6.722	10.845	10.845	0.662	4.785

In order to evaluate the denoising ability of the proposed fusion method, the same experiment is implemented on ‘Pepsi’ image added artificial noise (mean=0, variance=0.004) again. **Fig. 7(c)–(f)** are parts of corresponding region taken from fusion results, which are used to illustrate the denoising ability of the different methods. It can be seen that the region of bar code is immersed noise in **Fig. 7(c)–(e)**. On the contrary, the edges information is clearer and less noise in **Fig. 7(f)**. These fusion methods only consider the salient information, which leads noises may be transferred to fusion result in error. The directional vector is used in proposed fusion method. So, the **Fig. 7(f)** can reduce the noise to some extent. **Table 3** gives the quantitative results of **Fig. 7**. *PSNR* is used as the measure to verification denoising ability of these method. From **Table 3** we observe that the proposed scheme provides the best performance and outperforms other three image fusion method with larger MI, $Q^{AB/F}$, *PSNR*.

$$PSNR = 10 \times \log\left(\frac{255^2}{MSE}\right) \quad (24)$$

$$MSE = \frac{1}{mn} \sum_{i=0}^{m-1} \sum_{j=0}^{n-1} \|F(i, j) - I^A(i, j)\|^2 \quad (25)$$

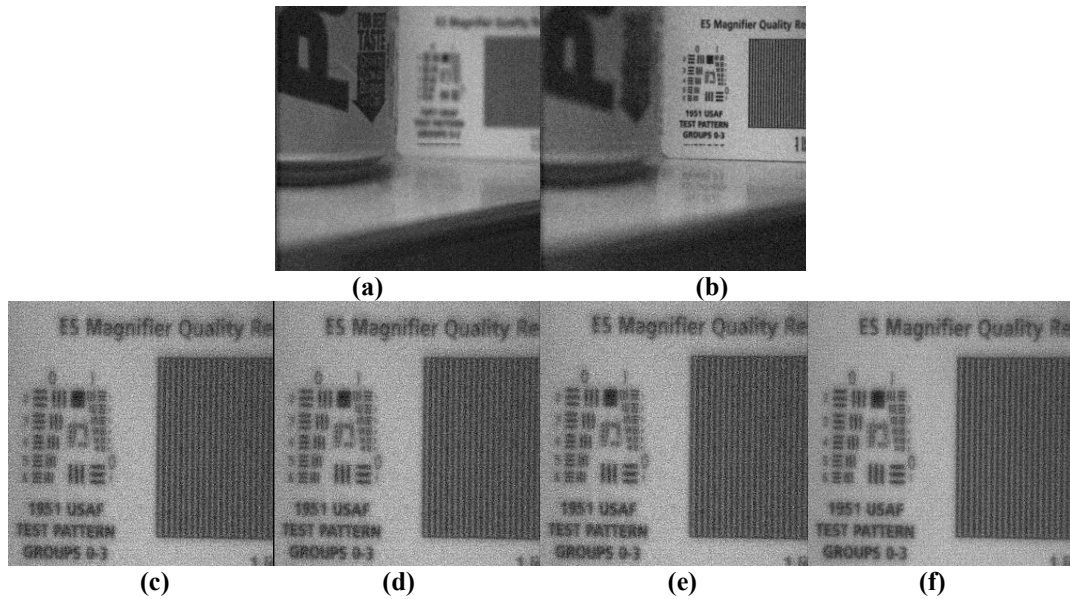


Fig. 7. The noisy image fusion results of different highpass coefficient fusion algorithms: (a)-(b) are the multifocus image paris with artificial noise; We only take parts region of the result to shown in (c)-(f), which are attained by the same fusion methoed used in Fig.6; (f) is porposed fusion method.

Table 3. Performance of the different fusion methods on noisy image Fig. 7(a) and (b),

Fusion rule	entropy	Q^{AF}	Q^{BF}	$Q^{AB/F}$	SF	PNSR
Local contrast	3.167	13.472	13.472	0.338	13.208	15.05
Local energy	3.152	13.475	13.475	0.329	13.244	15.07
Local variance	3.153	13.471	13.471	0.330	13.234	15.08
Proposed	3.221	13.456	13.456	0.3480	13.404	15.14

5.3 Comparisons on MSD Methods

The third experiment is performed on mul-tifocus clean images, the fused result of multi fusion algorithms is shown in Fig.6. In three algorithm, the lowpass which include the fusion algorithm based on DWT, the fusion algorithm based on CT and the proposed algorithm. The ‘average scheme’ and the ‘abs-maximum scheme’ are used in lowapss subband and the bandpass subband coefficients respectively in DWT and CT. In the last experiment, the proposed highpass subband fusion rule and the directional vector constraint local contrast is used in lowpass and highpass subband, respectively.

Fig. 8(a) is the fusion result by DWT-based decomposition. **Fig.8(b)** is the fused result by CT-based decomposition. **Fig.8(c)** is the fused result of the proposed algorithm with the NSCT-based decomposition. From visual effects, **Fig.8(c)** has the better visual quality than **Fig.8(a)** and **Fig.6(b)**. In **Fig.8(c)**, artifacts near the white books was dispared for the effective presentation edges and salient features of image by NSCT. In **Fig.8(a)** and **Fig.8(b)**,the pseudo-Gibbs is appeared in region near the connection of clock and wall for the wavelet and CT lacking shift-invariance. However, this phenomenon is eliminated in **Fig.8(c)**. Furthermore, the quantitative results of the MI, $Q^{AB/F}$ and SF value for different image fusion methods are given in **Table 4**. The data in **Table 3** sh1ows that MI, $Q^{AB/F}$ and SF of proposed algorithm is higher than the other two algorithms. All of these indicate that the proposed method are with higher performance in fusion.

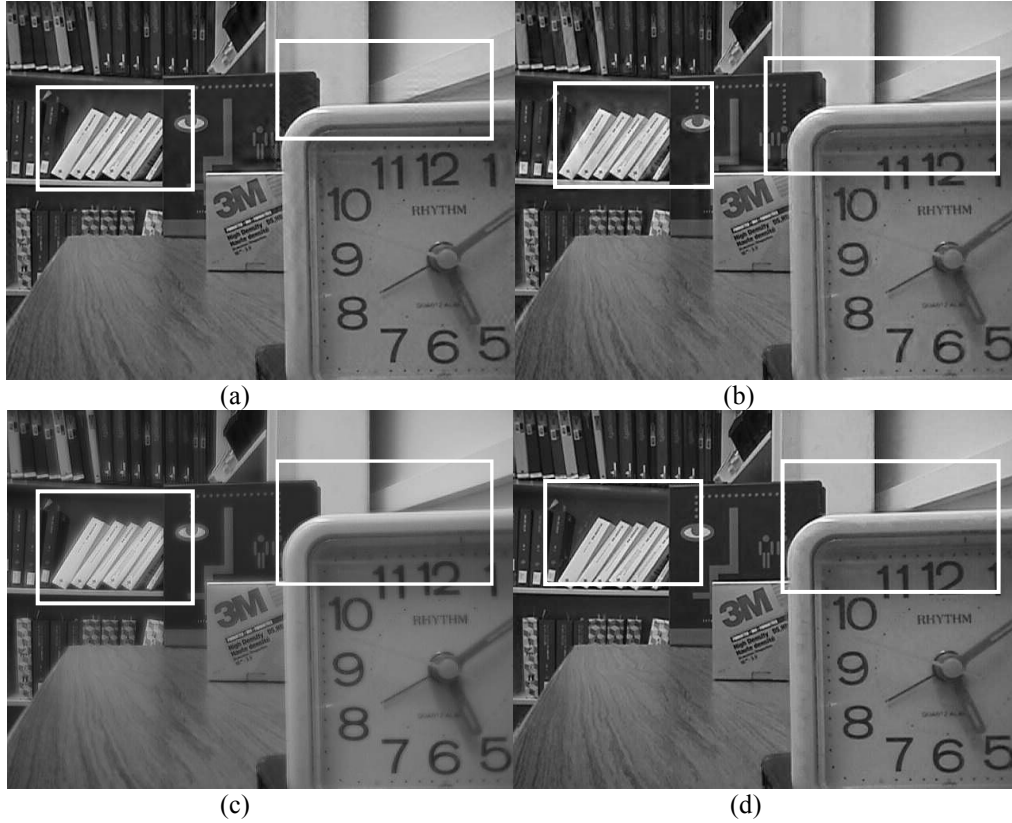


Fig. 8. Multifocus image fusion results of MSD-based methods, (a) fused images using DWT, (b) fused images using CT, (c) fused images using NSCT (d) fused images using proposed NSCT.

Table 4. Performance of the different fusion methods on processing Fig.7

MSD	entropy	Q^{AF}	Q^{BF}	$Q^{AB/F}$	SF
Wavelet	5.300	12.100	12.100	0.631	6.087
CT	5.521	11.993	11.993	0.632	5.895
NSCT	5.645	11.205	11.23	0.655	5.246
Proposed NSCT	7.456	11.351	11.351	0.721	6.111

6. Conclusion

In this paper, we firstly analyze the difference of multiresolution decomposition tools. The wavelet-based decomposition is limited to finite direction for representation of image information. So reconstructed image from the decomposed subband image will lose some detailed information and the pseudo-edge and block-effect will be appeared in fused image. The contourlet-based decomposition represents the structural information of image in multidirection, but do not have the shift-invariance. So, the frequency aliasing will appear in fused image reconstructed from the decomposed subband image. As a new multiscale geometric decomposition tool, the NSCT, with shift-invariance, multiresolution, multidirectional decomposition, multiscale and localization is more suitable for image fusion.

A novel multifocus image fusion algorithm based on NSCT is proposed in this paper. According to the characteristics of the human vision system and the perfect property of the coefficient decomposed by NSCT, A local multi-direction invariance (LEOV) represented the energy of image is used for fusion the lowpass subband coefficient. For highpass subband coefficients, a modified local features contrast is constrained by direction vector of coefficients is used to select the highpass subband coefficients. The proposed fusion method can prevent artifacts and erroneous introduced into the fused image and eliminate the 'block effect' and 'frequency aliasing' phenomenon. The experimental results on several pairs of multifocus images have demonstrated the superior performance of the proposed fusion scheme. The proposed algorithm not only can capture the more feature of image in lowpass coefficient, but also can introduce more visual detail form highpass coefficients, and employ the direction vector to attain the natural fused result. In addition, the direction vector can exclude the noise be selected into the fused image. The MST is effective sparse presentation for image, in which, compressed sensing is a new MST technique. The application of this theory for image fusion is our the next research in future.

Acknowledgments

This research was supported by the National Natural Science Foundation 60736046.

References

- [1] Yi Chai, Huafeng Li b, Zhaofei Li, "Multifocus image fusion scheme using focused region detection and multiresolution," *Optics Communications*, vol. 10, no. 19, pp.4376- 4389, September, 2011. [Article \(CrossRef Link\)](#).
- [2] Wei Huang,Zhongliang Jinga,"Evaluation of focus measures in multi-focus image fusion,"*Patter Recognition Letters*, vol.28, no.4, March 2007, pp.493-500.[Article \(CrossRef Link\)](#).
- [3] G. Salvador, C. Gabriel," On the use of a joint spatial-frequency representation for the fusion of multi-focus images," *Pattern Recognition Letters*, 26 (16) (2005) 2572. [Article\(CrossRefLink\)](#).
- [4] Qiang Zhanga,Bao-long Guob, "Multifocus image fusion using the nonsubsampling contourlet transform," *Signal Processing*, vol.89, No.7, July 2009, pp.1334-1346. [Article \(CrossRef Link\)](#).
- [5] Prabhu, V. and S. Mukhopadhyay, "A multi-resolution image fusion scheme for 2D images based on wavelet transform" in Recent Advances in Information Technology (RAIT), 2012 1st International Conference on: IEEE, pp. 80 – 85, March 2012. <http://ieeexplore.ieee.org/search/searchresult.jsp?newsearch=true&queryText=A+multi-resolution+image+fusion+scheme+for+2D+images+based+on+wavelet+transform&x=19&y=20>
- [6] Zhao, H., et al., "Multi-focus image fusion based on the neighbor distance," *Pattern Recognition*, vol 46, no.3, pp.1002-1011, March 2013. [Article \(CrossRef Link\)](#).
- [7] Wang, Z., Y. Ma, and J. Gu, "Multi-focus image fusion using PCNN," *Pattern Recognition*, vol.43, no.6: pp. 2003-2016, June, 2010. [Article \(CrossRef Link\)](#).
- [8] H.A. Eltoukhy, S. Kavusi, "A computationally efficient algorithm for multi-focus image reconstruction," in *Proc. of SPIE. Electronic Imaging*, pp. 332-341, January, 2003. [Article \(CrossRef Link\)](#).
- [9] G. Pajares, J. Cruz, "A wavelet-based image fusion tutorial," *Pattern Recognition*, vol.37, no. 9, pp.1855-1872, Sep, 2004. [Article \(CrossRef Link\)](#).
- [10] I. De, B. Chanda, "A simple and efficient algorithm for multifocus image fusion using morphological wavelets," *Signal Process*, vol. 86, no. 5, pp. 924-936, May, 2006. [Article \(CrossRef Link\)](#).
- [11] A. Toet, "Image fusion by a ratio of low-pass pyramid," *Pattern Recogn.Lett*, vol. 9, no 3, pp.

- 245-253, May, 1989. Article (CrossRef Link).
- [12] Li, S. and B. Yang, "Multifocus image fusion by combining curvelet and wavelet transform," *Pattern Recognition Letters*, 29(9): pp. 1295-1301, 2008. [Article \(CrossRef Link\)](#).
- [13] P.J. Burt, E.H. Adelson, "The Laplacian pyramid as a compact image code," *IEEE Transactions on Communications*, vol. 31, no. 4, pp. 532-540, Apr, 1983. [Article \(CrossRef Link\)](#).
- [14] T. Pu, G. Ni, "Contrast-based image fusion using the discrete wavelet transform," *Optical Engineering*, vol. 39, no. 8, pp. 2075-2082, Jul, 2000. [Article \(CrossRef Link\)](#).
- [15] P.J. Burt, "A gradient pyramid basis for pattern-selective image fusion," *Soc. Inform. Display Digest Tech. Papers* 16 (1985) 467-470. <http://www.google.com.hk/patents?hl=zh-CN&lr=&vid=USPAT5325449&id=OP0gAAAAEBAJ&oi=fnd&dq=%5B15%5D%09P.J.+Burt,+%E2%80%9CA+gradient+pyramid+basis+for+patter+n-selective+image+fusion&printsec=abstract#v=onepage&q&f=false>
- [16] G. Pajares, J. Cruz, "A wavelet-based image fusion tutorial," *Pattern Recognition*, vol. 37, no. 9, pp. 1855-1872, Sep, 2004. [Article \(CrossRef Link\)](#).
- [17] M.N. Do, M. Vetterli, "The contourlet transform: an efficient directional multiresolution image representation," *IEEE Transactions on Image Processing*, vol. 14, no. 12, pp. 2091-2106, Dec, 2005. [Article \(CrossRef Link\)](#).
- [18] A.L. da Cunha, J.P. Zhou, M.N. Do, "The Nonsubsampled Contourlet Transform: heory, Design, and Applications," *IEEE Transaction on Image Processing*, vol. 15, no. 12, pp. 3089- 3101, Oct, 2006. [Article \(CrossRef Link\)](#)
- [19] R. H. Bamberger and M. J. T. Smith, "A filter bank for the directional decomposition of images: Theory and design," *IEEE Trans. Signal Process.*, vol. 40, no. 4, pp. 882-893, Apr. 1992. [Article \(CrossRef Link\)](#)
- [20] R. R. Coifman and D. L. Donoho, "Translation invariant de-noising," in *Wavelets and Statistics*, A. Antoniadis and G. Oppenheim, Eds. New York: Springer-Verlag, 1995, pp. 125-150. [Article \(CrossRef Link\)](#)
- [21] Asmare, M.H., V.S. Asirvadam, and L. Iznita, "Multi-sensor image enhancement and fusion for vision clarity using contourlet transform," in *Proc of Information Management and Engineering, 2009. ICIME'09. International Conference on. 2009: IEEE*. pp:352-356, April 2009. http://ieeexplore.ieee.org/xpl/login.jsp?tp=&arnumber=5077056&url=http%3A%2F%2Fieeexplore.ieee.org%2Fxppls%2Fabs_all.jsp%3Farnumber%3D5077056
- [22] M. J. Shensa, "The discrete wavelet transform: Wedding the à trous and Mallat algorithms," *IEEE Trans. Signal Process.*, vol. 40, no. 10, pp. 2464-2482, Oct. 1992. [Article \(CrossRef Link\)](#)
- [23] R.H. Bamberger, M.J.T. Smith, "A filter bank for the directional decomposition of images: theory and design," *IEEE Transactions on Signal Processing*, vol. 40, no. 4, pp. 882-893. Apr, 1992. [Article \(CrossRef Link\)](#).
- [24] M. A. U. Khan, M. K. Khan, and M. A. Khan, "Coronary angiogram image enhancement using decimation-free directional filter banks," *In Proc. Int. Aoustics, Speech, and Signal Processing*, pp. 441-444, May 7-21, 2004. [Article \(CrossRef Link\)](#).
- [25] Yi Chaia, Huafeng Li, Xiaoyang Zhang, "Multifocus image fusion based on features contrast of multiscale products in nonsubsampled contourlet transform domain," *Optik- International Journal for Light and Electron Optics*, vol. 123, no. 7, pp. 569- 581, April, 2012. [Article \(CrossRef Link\)](#).
- [26] HuiLi, "Multi-sensor image fusion using the wavelet transform,". <http://ieeexplore.ieee.org/xpl/articleDetails.jsp?tp=&arnumber=413273&contentType=Conference+Publications&queryText%3DMulti-sensor+image+fusion+using+the+wavelet+transform>
- [27] A. Toet, L.J. van ruyven, J.M. Valetton, "Merging thermal and visual images by a contrast pyramid," *Optical Engineering*, v 28, n 7, p 789-792, Jul 1989. <http://opticalengineering.spiedigitallibrary.org/article.aspx?articleid=1223580%20>
- [28] Jianping Zhou, Arthur L. Cunha, and Minh N. Do, "NONSUBSAMPLED CONTOURLET TRANSFORM: CONSTRUCTION AND APPLICATION IN ENHANCEMENT," in *Proc. of IEEE Conf. IEEE International Conference on Image Processing*, pp.469-472, Sept 11-14, 2005 [Article \(CrossRef Link\)](#) .

- [29] G. Qu, D. Zhang, P. Yan, "Information measure for performance of image fusion," *Electron. Lett.* Vol. 38, no. 7, pp. 313-315, Mar, 2002. [Article \(CrossRef Link\)](#).
- [30] V. Petrovic, C. Xydeas, "On the effects of sensor noise in pixel-level image fusion performance," in *Proc. of 3th International Conference on Image Fusion*, pp. 14–19, May, 2002 [Article \(CrossRef Link\)](#)
- [31] Shutao Li, Bin Yang, Jianwen Hu, "Performance comparison of different multi-resolution transforms for image fusion," *Information Fusion*, vol. 12, no. 2, pp. 74–84, April, 2011. [Article \(CrossRef Link\)](#).



Cuiyin Liu received the MS degrees from the Southwest JiaoTong University, Chengdu, China, in 2007. Since 2009, she has been working towards the Ph.D. degree in school of computer science in Sichuan University. Her research interests include, image segmentation, image registration, image fusion and virtual reality. She is a member of the ACM.



Peng Cheng received BS degree from University of Electronic Science and Technology of China, Chengdu, China, in 2008. He is currently a Phd candidate in school of computer science in Sichuan University, Chengdu, China. His research interests include image registration, image fusion and computer vision.



Shu-qing Chen received her M.S. degree from South-central University for nationalities, China in 2005. Currently, she is working for her Ph.D degree in Sichuan University and also a lecturer with the Department of Electronics and Information Engineering in Putian University, China. Her research interests include image & video feature extraction, matching and alignment, and reconstruction. E-mail: talk2csq@hotmail.com



Cuiwei Wang received the MS degrees from the Southwest JiaoTong University, Chengdu, China, in 2006. Since 2006, she has been working in Computer Center, Kunming Univ. of Science and Tech. Her research interests include, image fusion, computer vision. 394116576@qq.com



Fenghong Xiang Kunming University of Science and Technology Professor, Dr. Master Instructor. Graduated from Kunming Institute of Technology Department of Automation. xiangfh5447@sina.com